Inorganic Chemistry

Communication

pubs.acs.org/IC

Regular High-Nuclearity Species from Square Building Blocks: A Triangular 3 × [2 × 2] Ni_{12} Complex Generated by the Self-assembly of Three [2 × 2] Ni_4 Molecular Grids

Yurii S. Moroz,[†,‡] Serhiy Demeshko,[§] Matti Haukka,[⊥] Andriy Mokhir,[¶] Utpal Mitra,[∥] Michael Stocker,[∥] Paul Müller,[∥] Franc Meyer,[§] and Igor O. Fritsky*[,†]

[†]Department of Chemistry, Kiev National Taras Shevchenko University, 64 Volodymyrska Street, 01601 Kiev, Ukraine

[§]Institute of Inorganic Chemistry, Georg-August-University Göttingen, Tammannstrasse 4, D-37077 Göttingen, Germany

[⊥]Department of Chemistry, University of Joensuu, P.O. Box 111, 80101 Joensuu, Finland

[¶]Institute of Inorganic Chemistry, Ruprecht-Karls-University Heidelberg, Im Neuenheimer Feld 270, D-69120 Heidelberg, Germany

[∥]Department of Physics, University of Erlangen-Nürnberg, Erwin-Rommel-Strasse 1, D-91058 Erlangen, Germany

Supporting Information

ABSTRACT: A dodecanuclear 3 × [2 × 2] nickel(II) complex has been obtained via the self-association of three tetranuclear [2 × 2] molecular grids. X-ray diffraction shows a "propeller-like" structure of the $[Ni_4]_3$ scaffold with a central μ_3-hydroxide. The dodecanuclear species remains stable in solution and can be deposited without decomposition on highly ordered pyrolytic graphite surfaces.

In recent years, efforts of reducing the dimensions of electronic devices to the nanoscale level have led to the development of increasingly complex molecule-based materials with promising switching, logic, and data-storage functions.[1] In the case of metal-containing molecule-based compounds, two alternative synthetic strategies are usually followed: one of them is based on the principles of molecular design, which allows strict control of the topology and nuclearity of new complexes. The main disadvantage of this method is associated with often complicated and multistage ligand syntheses. A different approach relies on spontaneous self-assembly processes, which usually take place upon the combination of relatively simple ligand molecules and metal ions and may lead to the formation of high-nuclearity species; however, it often is difficult to predict the exact topology and nuclearity of the products. A rational alternative that amalgamates both strategies is aggregation by the controlled self-assembly of well-defined supramolecular synthons with intermediate nuclearity, prepared in a first step. The subsequent self-association process of those synthons requires that the oligonuclear complexes are properly designed and feature functional groups that allow them to serve as building blocks for the final nanoscale frameworks.

Among the variety of metallosupramolecular arrays, grid-type metal-ion structures attract a lot of attention in this context.[2] A large number of square [$n \times n$] and rectangular [$n \times m$] molecular grids ($n, m = 2-4$) have meanwhile been reported.[2,3] They are usually based on strand-type ligands that provide linear sequences of bidentate and/or tridentate binding sites in combination with different metal ions that favor tetrahedral or octahedral coordination geometry, and they are usually formed via controlled self-assembly processes.[2] In most cases, the molecular grids use to be "closed entities" and thus do not have the possibility of aggregation via intergrid linkages because (a) metal ions in the grids do not have vacant sites or labile ligands (H_2O, etc.) and (b) the complexes do not contain any noncoordinated (and potentially bridging) donor groups or atoms at the grid rim. Therefore, previous examples of the formation of aggregates from such "grid bricks" relied on the presence of additional donor groups at the ligand periphery to generate solid-state polymeric architectures ("grids of grids") upon the addition of further metal ions (such as Ag^+).[4]

This Communication now describes the synthesis and investigation of a novel 3 × [2 × 2] Ni_{12} complex composed of three [2 × 2] molecular squares as building units. Previous studies on the easy-to-prepare polydentate strand-type ligand 2-(hydroxyimino)-N'-[1-(2-pyridyl)ethylidene]-propanohydrazone (**Hpop**; Scheme 1), which features a flexible hydrazone backbone, have shown that **pop** readily forms robust homo- and heterometallic Cu_4, Ni_4, and Cu_2Mn_2 [2 × 2] molecular grids.[5] The μ-O^{amide} group in those grids spans adjacent metal ions and was shown to efficiently mediate magnetic coupling, either ferromagnetic or antiferromagnetic depending on the metal-ion combination.[5] Two structural features in the previous **pop**-based [2 × 2] grids are noteworthy, namely, the presence of monodentate terminal $HCOO^-/HCOOH$, CH_3COO^-, or water ligands and the presence of noncoordinating O^{oxime} atoms of the **pop** strands, both located at the grid periphery. Because it is well-known that

Scheme 1. Structure of Hpop

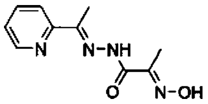

Received: May 3, 2012
Published: July 5, 2012

oxime groups may bridge metal ions,[6] we reasoned that intergrid connections may be formed under suitable reaction conditions upon substitution of the monodentate terminal ligands by O^{oxime} donors. This should result in high-nuclearity species from the parent "[2 × 2] grid bricks".

In accordance with these considerations, the reaction between H**pop** and $Ni(NO_3)_2{\cdot}6H_2O$ in a MeOH/H_2O solution with the addition of an excess of alkali (pH ∼ 8−9) resulted in the formation of a dark-brown solution, from which brown crystals of $[Ni_{12}(\mathbf{pop}\text{-H})_8(\mathbf{pop})_4(OH)(H_2O)_3](NO_3)(OH)_2{\cdot}nH_2O$ (**1**) were obtained in 68% yield. A single-crystal diffraction study shows that **1** consists of an assembly of three [2 × 2] molecular grids, each composed of four ligand strands and four Ni^{II} ions. The molecular structure of the dodecanuclear cation is shown in Figure 1; a core structure representation showing only the metal ions and the immediate ligand donor atoms is depicted in Figure S2 (Supporting Information, SI). The Ni_{12} array of **1** can be described as a "threefold propeller", where each "blade" is formed by an individual [2 × 2] Ni_4 unit. The grids are connected via deprotonated μ-(N,O) oxime groups from two orthogonal **pop**-H ligand strands of each Ni_4 subunit, hence by a total of six μ-(N,O) oxime bridges, and by a central μ_3-hydroxide. The hydroxide is located on a (noncrystallographic) pseudo-C_3 axis at the propeller hub. Each Ni^{II} ion per Ni_4 subunit has a distinct distorted octahedral coordination sphere: a $\{N_4O_2\}$ donor environment for Ni1, Ni7, and Ni11, $\{N_2O_4\}$ for Ni3, Ni5, and Ni9, and $\{N_3O_3\}$ for Ni2, Ni6, and Ni12 as well as for Ni4, Ni8, and Ni10. Ni···Ni′ separations within the Ni_4 squares are close to 4 Å, and the Ni−O−Ni′ angles fall in the range 136−142° (Table S1 in the SI). All Ni−O and Ni−N bond lengths as well as angles N−Ni−N′, O−Ni−N, and O−Ni−O′ are in common ranges for octahedral Ni^{II} with amide, pyridine, and oxime donors.[7] Ni−O and Ni−N bond lengths are quite similar for Ni^{II} ions of the hydroxide-centered Ni_3 core (Ni3, Ni5, and Ni9) and peripheral Ni^{II} ions. All amide groups are deprotonated. The presence of eight deprotonated and four protonated oxime groups of the ligand strands (**pop**-H vs **pop**) is evident from the X-ray data (Table S1 in the SI); all protonated oxime groups form hydrogen bonds with coordinated water molecules.

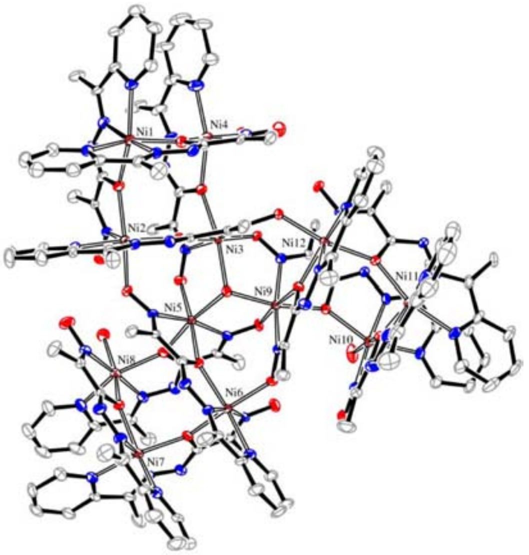

Figure 1. ORTEP-3 projection of the cation of **1** (blue, N; red, O, gray, C). H atoms are omitted for clarity (40% probability thermal ellipsoids).

The magnetic properties of **1** (Figure 2) reveal a decrease of $\chi_M T$ upon a lowering of the temperature, suggesting dominant antiferromagnetic interactions within the dodecanuclear aggregate. The room temperature value of $\chi_M T$ (10.8 cm^3 K mol^{-1}; 0.9 cm^3 K mol^{-1} per ion) is less than what is expected for an uncoupled Ni$^{II}{}_{12}$ system. Field-dependent magnetization studies at 2 K showed that M does not reach saturation (but a value of 1.54 $N\beta$) at 5 T (Figure S3 in the SI). Thus, the field- and temperature-dependent magnetic data suggest global antiferromagnetic coupling and an $S_T = 0$ ground state.

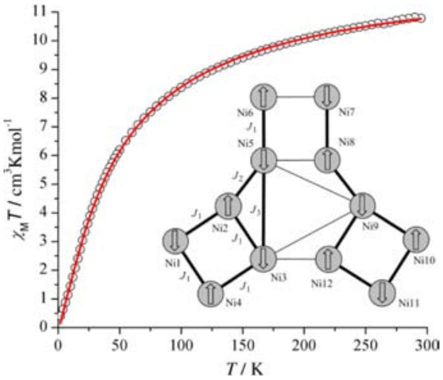

Figure 2. Magnetic data for **1** as a plot of $\chi_M T$ vs T. The solid line represents the best curve fit. The inset shows a schematic drawing of proposed magnetic exchange pathways in **1**.

It was shown previously that μ-O^{amide} bridges mediate weak antiferromagnetic coupling (J = −5 to −8 cm^{-1}) in [2 × 2] Ni$^{II}{}_4$ grids,[5a,7b] while single μ-(N,O)^{oxime} bridges give rise to moderate antiferromagnetic coupling (∼−15 cm^{-1}) between Ni^{II} ions.[8] Because simulations for the complete Ni_{12} core exceed common computational capabilities, we provisionally consider a hexanuclear fragment as a simplified model for magnetic data analysis (bold lines in the inset of Figure 2). It comprises three exchange parameters J that describe the different coupling pathways (assuming that the coupling along all four edges of [2 × 2] Ni_4 subunits is equivalent, for simplicity): coupling via μ-O^{amide} (J_1), via μ-(N,O)^{oxime} (J_2), and via μ_3-OH and μ-(N,O)^{oxime} bridges (J_3). While this will not provide exact values for the individual linkages, it gives an estimate of the magntidue of the exchange coupling for the Ni_{12} cation.[9] Similar simplifications have been previously applied for analyzing the susceptibility data of some polynuclear complexes.[4b] In view of the magnetostructural correlations mentioned above, we thus anticipated two antiferromagnetic (J_1 and J_2) and one ferromagnetic (J_3) components for **1**.

The appropriate spin Hamiltonian for isotropic exchange and Zeeman splitting in the simplified scheme is

$$\hat{H} = -2J_1(\hat{S}_1{\cdot}\hat{S}_2 + \hat{S}_2{\cdot}\hat{S}_3 + \hat{S}_3{\cdot}\hat{S}_4 + \hat{S}_1{\cdot}\hat{S}_4 + \hat{S}_5{\cdot}\hat{S}_6) - 2J_2\hat{S}_2{\cdot}\hat{S}_5 - 2J_3\hat{S}_3{\cdot}\hat{S}_5 + \sum_{i=1} g_i\mu_B B\hat{S}_{iz}$$

with $S_1 = S_2 = S_3 = S_4 = S_5 = S_6 = 1$. Simulation of the experimental data[8] gave $g_{av} = 2.11$, $J_1 = -4.9$ cm^{-1}, $J_2 = -6.1$ cm^{-1}, $J_3 = 5.2$ cm^{-1}, TIP = 0.2 × 10^{-4} cm^3 K mol^{-1}, ρ = 7.7% (S = 1), $\lambda = -4.1$ cm^{-3} mol, and $R = 6.2 \times 10^{-3}$ (TIP = temperature-independent paramagnetism, ρ = Curie-behaved paramagnetic monomer impurities, λ = molecular-field parameter, and $R = \{\sum[(\chi_MT)_{obs} - (\chi_MT)_{calc}]^2/\sum(\chi_MT)_{obs}{}^2\}^{1/2}$); we assume that λ includes contributions from all three coupling constants. The best fit using those parameters is illustrated as the red solid line in Figure 2. J values are in reasonable agreement with the above considerations (J_1 and J_2 reflecting antiferromagnetic coupling and J_3 reflecting the ferromagnetic interaction at the μ_3-hydroxide-centered core). The negative sign of λ indicates predominant antiferromagnetic coupling between the two hexanuclear fragments of the dodecanuclear cation.

The behavior of **1** in a MeOH/H_2O solution was investigated by electrospray ionization mass spectrometry (ESI-MS). A characteristic signal for a doubly charged ion at m/z 1670.5 is assigned to the species $[Ni_{12}(\mathbf{pop}\text{-}H)_9(\mathbf{pop})_3(OH)]^{2+}$ (M_{calc} = 3340.88), based on a reasonable agreement of the isotopic distribution pattern (see Figure S1 in the SI). This suggests that the integrity of the 3 × [2 × 2] dodecanuclear complex is retained in solution. In order to visualize individual nanoscale Ni_{12} molecules, a dilute solution of **1** was deposited onto a freshly cleaved surface of highly ordered pyrolytic graphite (HOPG) and investigated by scanning tunneling microscopy (STM).[10] The Ni_{12} cations self-organize into well-ordered strands along defects of the HOPG surface (Figure 3, left). A high magnification (Figure 3, right) shows blobs with a size that is roughly consistent with the molecular dimensions determined by single-crystal X-ray crystallography. The black triangle in Figure 3 is the approximate shape of the Ni_{12} cation with a side length of 2.1 nm.

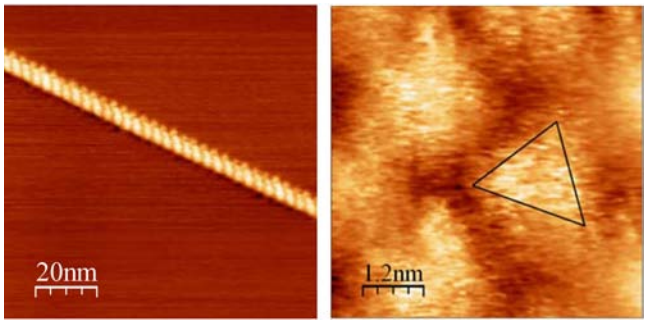

Figure 3. STM images of **1** deposited on HOPG. Left: Strand of molecules attached to a monatomic step of the HOPG. There are four molecules in parallel. Right: Magnification of the strand. The black triangle is the approximate shape of the Ni_{12} cation (Figure 1).

In summary, the formation of **1** represents the first example of the assembly of [2 × 2] grids into a triangular "propeller-like" dodecanuclear aggregate. The association process occurs because of the presence of accessible donor groups and labile ligands in the periphery of the individual Ni_4 squares. This demonstrates a promising strategy for the controlled synthesis of nanoscale objects from grid-type molecular components. The new Ni_{12} complex **1** can be nondestructively deposited on HOPG surfaces. While **1** shows dominant antiferromagnetic coupling and an S_T = 0 ground state, the self-assembly of related H**pop**-based (heterometallic) square building blocks with high-spin ground states, perhaps giving similar dodecanuclear complexes, may provide access to new-molecule-based materials with interesting properties. Work in that direction is in progress.

■ ASSOCIATED CONTENT

Ⓢ Supporting Information

Synthetic procedures, crystallographic details, and details of SQUID and ESI-MS measurements. This material is available free of charge via the Internet at http://pubs.acs.org.

■ AUTHOR INFORMATION

Corresponding Author

*E-mail: ifritsky@univ.kiev.ua.

Present Address

‡1-014 Center for Science and Technology, Department of Chemistry, Syracuse University, Syracuse, NY 13244-4100.

Notes

The authors declare no competing financial interest.

■ ACKNOWLEDGMENTS

Financial support from the State Fund for Fundamental Researches of Ukraine (Grant F40.3/041) is gratefully acknowledged. F.M. gratefully acknowledges financial support of this work by the DFG (SFB 602, project A16).

■ REFERENCES

(1) (a) Lehn, J.-M. *Supramolecular Chemistry. Concepts and Perspectives*; VCH: Weinheim, Germany, 1995. (b) Lehn, J.-M. *Science* **2002**, *295* (5564), 2400−2403. (c) Lehn, J.-M. *Proc. Natl. Acad. Sci. U.S.A.* **2002**, *99* (8), 4763−4768. (d) Service, R. F. *Science* **2003**, *302* (5645), 556−557+ 559.

(2) (a) Ruben, M.; Rojo, J.; Romero-Salguero, F. J.; Uppadine, L. H.; Lehn, J.-M. *Angew. Chem., Int. Ed.* **2004**, *43* (28), 3644−3662. (b) Dawe, L. N.; Shuvaev, K. V.; Thompson, L. K. *Chem. Soc. Rev.* **2009**, *38*, 2334−2359. (c) Stadler, A. M. *Eur. J. Inorg. Chem.* **2009**, 4751−4770.

(3) (a) Klingele, J.; Prikhod'ko, A. I.; Leibeling, G.; Demeshko, S.; Dechert, S.; Meyer, F. *Dalton Trans.* **2007**, 2003−2013. (b) van der Vlugt, J. I.; Demeshko, S.; Dechert, S.; Meyer, F. *Inorg. Chem.* **2008**, *47* (5), 1576−1585. (c) Schneider, B.; Demeshko, S.; Dechert, S.; Meyer, F. *Angew. Chem., Int. Ed.* **2010**, *49*, 9274−9277.

(4) (a) Ruben, M.; Ziener, U.; Lehn, J.-M.; Ksenofontov, V.; Gütlich, P.; Vaughan, G. B. M. *Chem.—Eur. J.* **2005**, *11*, 94−100. (b) Dawe, L. N.; Shuvaev, K. V.; Thompson, L. K. *Inorg. Chem.* **2009**, *48* (8), 3323−3341. (c) Shuvaev, K. V.; Dawe, L. N.; Thompson, L. K. *Eur. J. Inorg. Chem.* **2010**, 4583−4586.

(5) (a) Moroz, Y. S.; Kulon, K.; Haukka, M.; Gumienna-Kontecka, E.; Kozłowski, H.; Meyer, F.; Fritsky, I. O. *Inorg. Chem.* **2008**, *47*, 5656−5665. (b) Moroz, Y. S.; Szyrwiel, Ł.; Demeshko, S.; Kozłowski, H.; Meyer, F.; Fritsky, I. O. *Inorg. Chem.* **2010**, *49*, 4750−4752.

(6) Kanderal, O. M.; Kozlowski, H.; Dobosz, A.; Świątek-Kozłowska, J.; Meyer, F.; Fritsky, I. O. *Dalton Trans.* **2005**, 1428−1437.

(7) (a) Meyer, F.; Kozlowski, H. In *Comprehensive Coordination Chemistry II*; McCleverty, J. A., Meyer, T. J., Eds.; Elsevier: Oxford, U.K., 2004; Vol. *6*. (b) Matthews, C. J.; Avery, K.; Xu, Z. Q.; Thompson, L. K.; Zhao, L.; Miller, D. O.; Biradha, K.; Poirier, K.; Zaworotko, M. J.; Wilson, C.; Goeta, A. E.; Howard, J. A. K. *Inorg. Chem.* **1999**, *38*, 5266−5276.

(8) Azuah, R. T.; Kneller, L. R.; Qiu, Y.; Tregenna-Piggott, P. L. W.; Brown, C. M.; Copley, J. R. D.; Dimeo, R. M. *J. Res. Natl. Inst. Stand. Technol.* **2009**, *114*, 341.

(9) An alternative model that considers only the Ni_4 subunits (with a single J_1) gives $J_1 = -6.9$ cm^{-1} and $\lambda = -9.3$ cm^{-3} mol.

(10) Ruben, M.; Lehn, J.-M.; Müller, P. *Chem. Soc. Rev.* **2006**, *35*, 1056−1067.